Heike E. Daldrup-Link, MD
Martina Rudelius, MD
Robert A. J. Oostendorp, PhD
Marcus Settles, PhD
Guido Piontek, MS
Stefan Metz, MD
Hilkea Rosenbrock, PhD
Ulrich Keller, MD
Ulrich Heinzmann, MD, PhD
Ernst J. Rummeny, MD
Jürgen Schlegel, MD
Thomas M. Link, MD

Index terms:
Experimental study
Iron
Magnetic resonance (MR), contrast media
Magnetic resonance (MR), experimental studies, 57.121411, 57.121413
Molecular analysis
Stem cells

Published online before print
10.1148/radiol.2283020322
Radiology 2003; 228:760–767

Abbreviations:
DMEM = Dulbecco's modified Eagle's medium
SE = spin echo
SI = signal intensity
SPIO = superparamagnetic iron oxide
USPIO = ultrasmall SPIO

[1] From Dept of Radiology (H.E.D.L., M.S., S.M., E.J.R., T.M.L.), Inst of Pathology (M.R., G.P., U.H., J.S.), Third Clinic of Internal Medicine, Laboratory of Stem Cell Physiology (R.A.J.O., U.K.), Dept Clinical Chemistry and Pathochemistry (H.R.), and National Research Ctr for Environment and Health (U.H.), Technical Univ, Ismaninger Str 22, 81675 Munich, Germany. Received Apr 2, 2002; revision requested Jun 13; final revision received Oct 31; accepted Jan 14, 2003. Supported by German Research Foundation grant DA 529/1-1. **Address correspondence to** H.E.D.L. (e-mail: *daldrup@roe.med.tu-muenchen.de*).

Author contributions:
Guarantors of integrity of entire study, H.E.D.L., M.R., R.A.J.O.; study concepts, all authors; study design, H.E.D.L., M.R., R.A.J.O., U.K., M.S., J.S., T.M.L.; literature research, H.E.D.L., M.R., R.A.J.O., M.S.; experimental studies, H.E.D.L., M.R., R.A.J.O., M.S., G.P., S.M., H.R., U.H.; data acquisition, H.E.D.L., M.R., R.A.J.O., M.S., G.P.; data analysis/interpretation, H.E.D.L., M.R., R.A.J.O., H.R., U.H.; statistical analysis, H.E.D.L., T.M.L.; manuscript preparation, H.E.D.L., M.R., R.A.J.O.; manuscript definition of intellectual content, H.E.D.L., M.R., R.A.J.O., U.K., M.S., J.S., T.M.L.; manuscript editing, H.E.D.L., T.M.L.; manuscript revision/review and final version approval, all authors

Targeting of Hematopoietic Progenitor Cells with MR Contrast Agents[1]

PURPOSE: To label human hematopoietic progenitor cells with various magnetic resonance (MR) imaging contrast agents and to obtain 1.5-T MR images of them.

MATERIALS AND METHODS: Hematopoietic progenitor cells, labeled with ferumoxides, ferumoxtran, magnetic polysaccharide nanoparticles–transferrin, P7228 liposomes, and gadopentetate dimeglumine liposomes underwent MR imaging with T1- and T2-weighted spin-echo and fast field-echo sequences. Data were analyzed by measuring MR signal intensities and R1 and R2* relaxation rates of labeled cells and nonlabeled control cells. Mean quantitative data for the various contrast agent groups were assessed for significant differences compared with control cells by means of the Scheffe test. As a standard of reference, MR imaging data were compared with electron microscopic and spectrometric data.

RESULTS: For all contrast agents, intracellular cytoplasm uptake was demonstrated with electron microscopy and was quantified with spectrometry. When compared with nonlabeled control cells, progenitor cells labeled with iron oxides showed significantly ($P < .05$) increased R2*. Cells labeled with gadopentetate dimeglumine liposomes showed significantly increased R1. Detection thresholds were 5×10^5 cells for gadopentetate dimeglumine liposomes and ferumoxtran, 2.5×10^5 cells for ferumoxides and P7228 liposomes, and 1×10^5 cells for magnetic polysaccharide nanoparticles–transferrin.

CONCLUSION: Hematopoietic progenitor cells can be labeled with MR contrast agents and can be depicted with a standard 1.5-T MR imager.

Progress in the field of human stem cell transplantation has reduced transplant-related toxicities and has improved survival rates (1). To date, however, the rapidity and durability of stem cell graft placement can be measured only indirectly, on the basis of platelet and neutrophil counts from the peripheral blood (1). To our knowledge, direct in vivo visualization of transplanted cells is not yet established in humans. Magnetic resonance (MR) imaging contrast agents could be used to label hematopoietic cells to allow direct depiction of cellular traffic, homing in the bone marrow, differentiation of immature cells, and transplant rejection in vivo (2,3). Various investigators approached this problem and labeled various hematopoietic cell populations—including lymphocytes, monocytes, progenitor cells, and embryonic cells—with MR contrast agents (2–6).

Previously used MR contrast agents and labeling methods, however, are far from being approved for clinical applications. Furthermore, previous studies were often performed with MR systems with high field strength up to 14 T (2), whereas most clinical MR imagers are operated up to 1.5 T. These previous labeling methods were used to optimize the detectability of minimal cell numbers, which may not be a practical drawback in the evaluation of hematopoietic stem cell transplants. In clinical practice, high cell numbers (eg, 2×10^8 progenitor cells per kilogram of body weight) are usually transplanted, and it is more important to follow up the majority population of the transplanted cells than it is to follow up single cells. Therefore, we focused on labeling methods that may be applicable in current clinical protocols and on MR contrast agents that are either approved by the U.S. Food and Drug Administration or are expected to be approved in the near future.

The purpose of this study was to label human hematopoietic progenitor cells with various MR contrast agents and to obtain 1.5-T MR images of them.

MATERIALS AND METHODS

Cell Suspensions

The study was approved by the institutional review board, and informed consent was obtained from the female donors before each stem cell collection. Suspensions of human hematopoietic progenitor cells were prepared from umbilical cord blood, which was collected from the umbilical cord vein after normal delivery of a full-term infant. Umbilical cord blood was collected in heparin-flushed syringes, stored at 4°C, and processed within 24 hours of collection. Low-density cells were isolated with density *(d)* centrifugation (d = 1.077 g/mL) (Biocoll; Biochrom, Berlin, Germany). After centrifugation at 1,000*g* for 20 minutes, the mononuclear interphase cells were collected and washed once in a balanced salt solution (Hanks; InvitroGen, Karlsruhe, Germany) supplemented with 2% fetal calf serum (Biochrom, Berlin, Germany) and 10 mmol/L 4-(2-hydroxyethyl)piperazine-1-ethane sulfonic acid, or HEPES, (Gibco, Karlsruhe, Germany). Subsequently, red cells were lysed with a reagent (Ortholysis; Ortho). After erythrolysis, the cell samples were washed twice in the salt solution. Before incubation with contrast agents, the cells were again centrifuged, and the cell pellet was resuspended with 1 mL of Dulbecco's modified Eagle's medium (DMEM) (Gibco). The number of cells was counted in a cell counter by two investigators (H.E.D.L., M.R.). Both investigators performed all counts independently. The mean of the two counts was used for data analysis before each experiment.

Contrast Media

MR contrast agents were selected to target cells by means of three mechanisms: fluid-phase endocytosis, receptor-mediated endocytosis, and transfection with liposomes.

Fluid-phase mediated endocytosis of iron oxides.—This endocytosis was achieved by incubating the cell suspensions with iron oxides.

Ferumoxides (Endorem; Laboratoire Guerbet, Aulnay-sous-Bois, France) is made of colloid-based superparamagnetic iron oxide (SPIO) particles with an R2/R1 ratio (in liters per millimole per second) of 160/40 and a diameter of 120–180 nm (mean, 150 nm) (7,8). Ferumoxides particles consist of nonstoichiometric magnetite cores, which are covered with a dextran T-10 layer (7,9). Ferumoxides is approved in the United States and Europe as an MR contrast agent that is specific to the reticuloendothelial system.

Ferumoxtran (Sinerem; Laboratoire Guerbet) is a prototype colloid-based ultrasmall SPIO (USPIO) that also represents iron oxide particles with a dextran layer (9). However, the particle diameter range of 20–50 nm (mean, 35 nm) is approximately four times smaller than that of ferumoxides. At 37°C and 0.47 T, R1 is 22 $L \times mmol^{-1} \times sec^{-1}$ and R2 is 80 $L \times mmol^{-1} \times sec^{-1}$ (9–11). Clinical approval of this agent is expected in Europe in 2004.

Receptor-mediated endocytosis of magnetic nanoparticles bound to transferrin.—Magnetic polysaccharide nanoparticles (Nanomag; Micromod, Rostock, Germany) have a diameter of 50 nm and contain approximately 35% magnetite and cross-linked dextran. Other than the previously mentioned iron oxides, these superparamagnetic nanoparticles are covalently bound to amino acid sequences that allow complex formation with metal ions and organic substances. For this study, magnetic polysaccharide nanoparticles were covalently bound to human transferrin, with a stoichiometry of 1.5 μmol of transferrin per 1 mg of iron (Fe) (ie, one magnetic polysaccharide nanoparticle bound to one transferrin molecule).

Transfection with anionic contrast agents in liposomes.—P7228 (Laboratoire Guerbet) is a new second-generation USPIO. Physicochemical characteristics, as well as R1 and R2, are similar to those of ferumoxtran, but P7228 particles are covered by an anionic dextran derivative instead of a dextran layer (9).

Gadopentetate dimeglumine (Magnevist; Schering, Berlin, Germany) is the standard MR contrast medium for clinical use. It has a molecular weight of 547 Da, and the molecules are approximately 100 times smaller than those of the previously mentioned iron oxides. R1 is 3.8 $L \times mmol^{-1} \times sec^{-1}$ (12,13).

As a result of their negative charge, P7228 particles and gadopentetate dimeglumine molecules can be encapsulated with positively charged liposomes. For this study, small unilamellar liposomes with a diameter of 100–200 nm were used to provide highly reproducible transfections by means of entrapment rather than encapsulation of anionic molecules (14). Two to four liposomes associate with a single contrast agent molecule or particle; then, the lipid complex fuses with the cell plasma membrane and delivers the contrast agent to the cell cytosol (14). Transfection was achieved as follows: 20 μL of liposome formulation (Lipofectin; InvitroGen), which contains 1:1 cationic lipid *N*-[1-(2,3-dioleyloxy)propyl]-*n*,*n*,*n*-trimethylammonium chloride and dioleoyl phosphatidylethanol-amine (14), were dissolved in 100 μL of DMEM and incubated at 37°C for 30 minutes with either P7228 or gadopentetate dimeglumine, each diluted in 100 μL of DMEM. These stock solutions were further diluted in 800 μL of DMEM.

Exposure of Cell Suspensions to MR Contrast Agents

Suspensions of hematopoietic progenitor cells were transferred to 1.5-mL tubes. Increasing cell numbers from 1×10^4 to 2×10^6 cells were exposed to the various contrast agents. Iron oxides were added at a dose of 250 μg Fe, P7228 liposomes at a dose of 100 μg Fe, and gadopentetate dimeglumine liposomes at a dose of 500 μg gadolinium per cell suspension. After exposure for 2, 4, 6, 8, and 24 hours, cells were centrifuged, the MR contrast agent containing supernatant was withdrawn, and cells were washed at least three times with DMEM. Cells were again centrifuged, and the cell pellets were evaluated at MR imaging. After the MR experiments, the cell probes were analyzed further by means of viability tests, spectrometry, and electron microscopy.

MR Imaging

MR imaging was performed with a clinical 1.5-T MR imager (Philips Medical Systems, Best, the Netherlands) and a high-resolution birdcage coil (Medical Advances, Milwaukee, Wis). To avoid susceptibility artifacts from the surrounding air in the images, all probes were placed in a plastic container filled with water. For pulse sequence optimization and subsequent calculation of reference R1 and R2 curves, reference samples of each contrast agent were imaged with increasing dilutions of iron oxides (0.122–250.000 μg Fe per milliliter) and gadopentetate dimeglumine (0.244–500.000 μg gadolinium per milliliter). Then, the test tubes with centrifuged cell pellets were imaged. Each subset of imaged progenitor cells contained labeled cells and nonlabeled control cells.

MR pulse sequences included T1- and

T2-weighted two-dimensional spin-echo (SE) and three-dimensional fast field-echo sequences. For measurements of R1, a mixed inversion-recovery SE sequence was initiated with an inversion-recovery experiment (repetition time msec/echo time msec/inversion time msec of 5,000/18/600) followed by an SE experiment (repetition time msec/echo time msec of 600/24). For measurements of R2*, a T2*-weighted fast field-echo echo-planar imaging sequence was performed with a repetition time of 2,000 msec, 20 increasing echo times from 4 to 36 msec, and a flip angle of 90°. Both sequences were performed with a field of view of 160 × 48 mm, a matrix of 256 × 256 pixels, and a section thickness of 1.5 mm. In addition, two-dimensional T1-weighted SE (500/15) and T2-weighted SE (2,500/100) sequences were performed with a field of view of 130 × 65 mm, a matrix of 256 × 256 pixels, two signals acquired, 17 sections, and a section thickness of 1.5 mm. Three-dimensional T1-weighted (25/2.7 with flip angle of 40°) and T2*-weighted (25/12 with flip angle of 20°) fast field-echo sequences were performed with a field of view of 200 × 160 mm, a matrix of 400 × 400 pixels, two signals acquired, and an effective section thickness of 1.5 mm. We did not perform fast SE sequences because they have a well-known lower sensitivity to iron oxides compared with that of conventional SE and gradient-echo sequences (7–11,15). MR imaging experiments were performed six times for each contrast agent.

In some experiments, one set of cells of each contrast agent, as well as nonlabeled control cells, were cultured after the initial MR examination. Cells were cultured in serum-free medium: 20% BIT, or BSA/insulin/transferrin (BIT9500; StemCell Technologies, Vancouver, British Columbia, Canada), 80% Iscove's modified Dulbecco's medium (Gibco), 10^{-4} mol/L β-mercaptoethanol, 40 μg of low-density lipoproteins (Sigma) and supplemented with the following growth factors: stem cell factor (100 ng/mL [R&D Systems, Minneapolis, Minn]), Fll2/Flt3 ligand (100 ng/mL [R&D Systems]), and thrombopoietin (20 ng/mL, [R&D Systems]). Follow-up MR studies were performed for up to 7 days.

Viability Tests

Cell viability was determined by means of exclusion with trypan blue dye. Progenitor cells (2.5×10^5) of each contrast agent, as well as nonlabeled control cells, were exposed to trypan blue dye, and the relative number of nonstained viable cells to the number of stained nonviable cells was calculated. These tests were performed four times for each contrast agent by an independent observer (R.A.J.O.), who was blinded to the labeling procedures.

Spectrometry

The iron concentration within cells labeled with the various iron oxide–based contrast agents was quantified with atomic absorption spectrometry by using a polarized atomic absorption spectrometer (Zeeman spectrometer model Z-8200; Hitachi, Tokyo, Japan). If necessary, the cell suspensions were diluted with 0.05 mol/L HCl. For iron measurements, the spectrophotometer was set to 248.3 nm and calibrated with six standards, which contained from 89.55 to 3,582 μmol/L Fe in 0.05 mol/L HCl. For quality control, normal and abnormal control cells (Lyphochek; Bio-Rad Laboratories, Munich, Germany) were used. Gadolinium concentration within the cells was measured with inductively coupled plasma atomic emission spectrometry.

Electron Microscopy

Hematopoietic cells (1×10^6) incubated with each of the contrast agents, as well as nonlabeled control cells, underwent MR imaging and subsequent evaluation with electron microscopy. These specimens were fixed in 3% glutaraldehyde-cocadylate buffer at 3°C overnight. Then, after 1 hour in 1% OsO_4, they were dehydrated in graded dilutions of ethanol, embedded in artificial resin (Epon; Merck, Darmstadt, Germany), and processed for electron microscopy. Thin sections of the cell probes were evaluated unstained (ie, without double staining with uranyl acetate and lead citrate) to prevent false-positive findings. In addition, probes of each contrast agent (without cells) were examined with electron microscopy to obtain a standard for the particles to be detected in the cells. Electron microscopy (EM 10 CR; Zeiss, Oberkochen, Germany) was performed at 60–80 kV. One investigator (U.H.) evaluated the cells for any structural changes as a result of the labeling procedure, as well as presence and localization of intracellular contrast agent particles.

Data Analysis

Mean signal intensities (SIs) for the cell pellets were measured in the central section of the imaging volume by one investigator (H.E.D.L.) with use of operator-defined regions of interest. The size of the regions of interest depended on the diameter of the cell pellets, with a minimum of 10 pixels per region. The SI data were divided by the background noise to yield the signal-to-noise ratio (SNR): SNR = SI/noise (16). The difference in SI (ΔSI) of labeled cells and nonlabeled control cells was calculated as $\Delta SI = (SI_{labeled\ cells} - SI_{controls})/noise$ (16).

T1 maps were used as calculated with the imager software without further modification, as described previously (17). On these maps, The T1s (in milliseconds) of labeled cells, which were derived by means of region-of-interest measurements of cell pellets on these maps, were converted to R1s (per second). For T2* mapping, the multiple-echo fast field-echo MR images were exported as digital imaging and communications in medicine, or DICOM, images to a personal computer with a Linux operating system. A self-written IDL program (Interactive Data Language; Research Systems, Boulder, Colo) was used to calculate R2* (per second) as the negative slope of the logarithm of the SIs, assuming a monoexponential decay of the free induction decay (18). Care was taken to analyze only data points with SIs that were significantly above the noise level. Thus, for the highest iron concentrations ($R2^* \geq 200\ sec^{-1}$), only the first three to five echo times could be used, which led to relatively large SDs in those cases.

Statistical Analysis

ΔSI data were presented as means and standard errors of the means. To compare differences in ΔSI data between various MR contrast agents and pulse sequences, analysis of variance for repeated measurements was used. Mean data were compared with the Scheffe test. Linear regression analysis was performed to compare iron uptake in the cells with increasing cell numbers and increasing incubation times. A *P* value of less than .05 was considered to indicate a statistically significant difference (Statview, version 4.1; Abacus, Berkeley, Calif).

RESULTS

Cell Viability and Electron Microscopy

Cell viability was not significantly impaired after 2 hours of exposure to any MR contrast agent. There was a tendency

TABLE 1
Results after 2-hour Exposure to MR Contrast Agents

Cells ($\times 10^6$)	MR Contrast Agent		Cell Pellet		Cell Viability (%)
	Added	Internalized	R2* (sec^{-1})	R1 (sec^{-1})	
Controls	None	0.001 ± 0.002 μg Fe	60.3 ± 4.4	0.57 ± 0.12	93.7 ± 5.1
Ferumoxides	250 μg Fe	2.4 ± 0.7 μg Fe*	144.1 ± 23.5†	8.14 ± 0.32*	90.4 ± 7.9
Magnetic polysaccharide nanoparticles–transferrin	250 μg Fe	9.8 ± 2.4 μg Fe‡	166.7 ± 29.5†	7.56 ± 0.45*	82.3 ± 12.4
Ferumoxtran	250 μg Fe	1.1 ± 0.4 μg Fe*	121.7 ± 7.3†	1.98 ± 0.24*	89.2 ± 8.1
P7228 liposomes	100 μg Fe	1.8 ± 0.5 μg Fe*	135.1 ± 19.4†	3.89 ± 0.37*	81.0 ± 11.1
Gadopentetate dimeglumine liposomes	40 μg Gd	12.5 ± 2.3 μg Gd†	83.5 ± 9.8	1.13 ± 0.14‡	80.6 ± 11.4

Note.—Data are ΔSI. Differences between control cells and MR contrast agent–labeled cells were analyzed. Gd = gadolinium.
* $P < .01$.
† $P < .05$.
‡ $P < .001$.

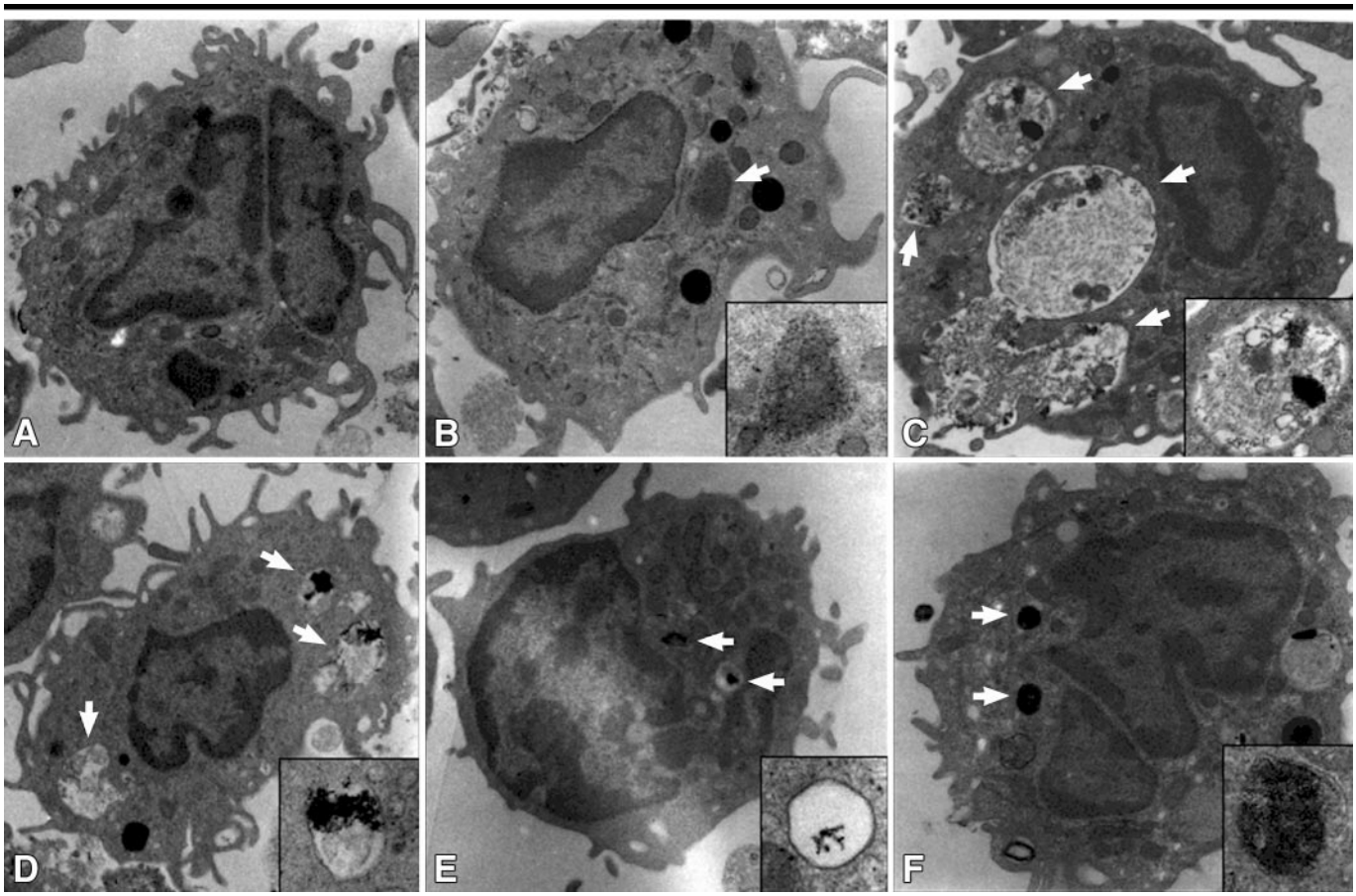

Figure 1. Electron microscopic images of hematopoietic progenitor cells. *A,* Nonlabeled control cell. *B–F,* Labeled cells are shown with inserts of contrast medium containing cytoplasmatic vesicles (which are not in all cases taken from the section of the image). In *B,* gadopentetate dimeglumine liposomes (arrow) are clustered within the cytoplasm. In *C–F,* intracellular accumulations of iron oxides form clusters in secondary lysosomes (arrows). The amount of internalized particles appears to be maximal for magnetic polysaccharide nanoparticles–transferrin *(C),* followed by ferumoxides *(D),* and ferumoxtran *(E).* In *F,* the relatively small amount of internalized P7228 can be increased substantially by means of transfection with liposomes.

toward slightly lower viability of cells after transfection with liposomes compared with that with the other labeling methods (Table 1).

Electron microscopy did not reveal any structural changes of labeled cells compared with nonlabeled control cells (Fig 1). Intracellular cytoplasmatic accumulation in vesicles was seen with all MR contrast agents. Iron oxide particles were preferentially localized in lysosomes. Gadopentetate dimeglumine liposomes were localized freely in the cytoplasm or near the Golgi apparatus.

Labeling Efficiency

Cellular uptake of iron oxides was highest for magnetic polysaccharide nanoparticles–transferrin, followed by ferumoxides, P7228 liposomes, and ferumoxtran, in decreasing order (Table 1).

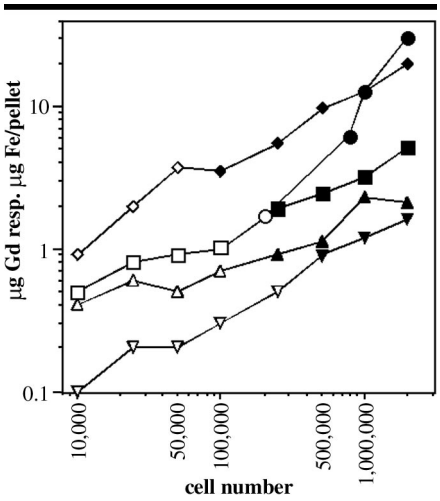

Figure 2. Curve depicts cellular uptake of MR contrast agents with increasing cell number, as quantified with spectrometry for iron oxides (micrograms of iron) and with inductively coupled plasma atomic emission spectrometry for gadopentetate dimeglumine (micrograms of gadolinium). ●, ○ = gadopentetate dimeglumine liposomes; ■, □ = ferumoxides; ▲, △ = P7228 liposomes; ▼, ▽ = P7228; and ◆, ◇ = magnetic polysaccharide nanoparticles. Solid keys = cell pellets visible on either T1- or T2-weighted MR images. Open keys = cell pellets that could not be detected at MR imaging.

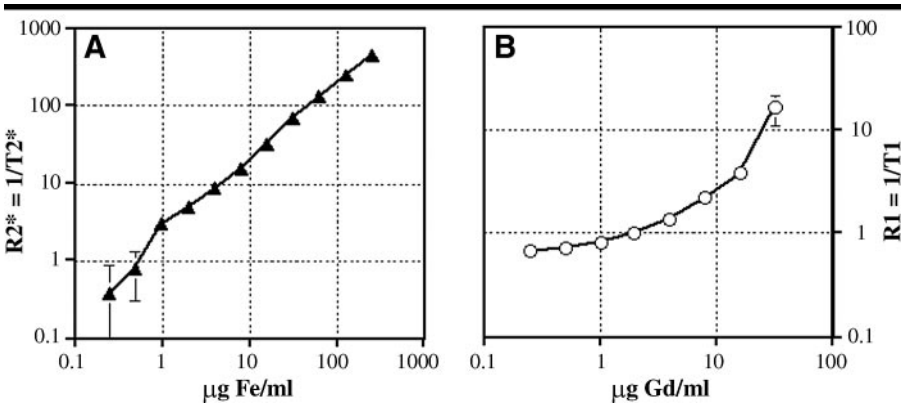

Figure 3. Validation curves of measurements as a function of contrast agent concentration in 1 mL of DMEM. *A,* T2* measurements. *B,* T1 measurements. In *A,* curve shows increasing concentrations (micrograms of iron) of P7228, as a representative iron oxide contrast agent, displayed against R2*, which was measured with a fast field-echo echo-planar MR imaging sequence. In *B,* curve shows increasing concentrations (micrograms of gadolinium) of gadopentetate dimeglumine displayed against R1, which was measured with a mixed inversion-recovery SE MR sequence.

Results of simple endocytosis of both USPIO, ferumoxtran and P7228, were not significantly different ($P > .05$), but there was a significant difference between USPIO uptake due to simple endocytosis and that due to the liposome-transfection method ($P < .05$). Compared with P7228 liposomes, gadopentetate dimeglumine liposomes accumulated in a higher quantity within the cells. The smaller size and stronger negative charge of the gadopentetate dimeglumine molecule may have facilitated the encapsulation with cationic liposomes, with subsequent improved transfection. The uptake of all MR contrast agents increased linearly with increasing cell numbers (Fig 2).

The iron oxide uptake could be increased with prolonged incubation times: for ferumoxides and ferumoxtran, the uptake increased linearly up to an incubation time of 24 hours ($r^2 = 0.86$ and 0.90, respectively). For receptor-mediated endocytosis of magnetic polysaccharide nanoparticles–transferrin, a plateau was reached after an incubation of 4 hours. For transfection with P7228 liposomes and gadopentetate dimeglumine liposomes, uptake was saturated after 2 hours. However, cell viability decreased with increasing incubation time. Therefore, an incubation time of 2–4 hours for all contrast agents was considered a good compromise between loading effectiveness and cell preservation.

MR Imaging

R1 and R2.*—Validation curves for the R1 and R2* measurements are shown in Figure 3. All cells labeled with iron oxide contrast agents showed significantly different R1 and R2* measurements compared with those for nonlabeled control cells ($P < .05$, Table 1). Even with very short inversion and echo times, R1 was dominated by R2*. In accordance with the iron oxide concentrations, R2* was maximal for cell pellets labeled with magnetic polysaccharide nanoparticles–transferrin, followed by ferumoxides, P7228 liposomes, and ferumoxtran (Table 1). After incubation with gadopentetate dimeglumine liposomes, cell pellets showed significantly different R1 and R2* values compared with those for nonlabeled control cells ($P < .05$, Table 1).

SI.—All cell pellets labeled with iron oxides showed a markedly decreased SI on T2-weighted MR images (Fig 4). On T1-weighted MR images, the SI was increased for ferumoxtran-labeled cells and decreased for cells labeled with the other iron oxides. As expected, ΔSI data were significantly different between T2*- and T1-weighted MR sequences ($P < .05$, Table 2, Fig 4). While the actual size of the cell pellet approximately matched the size of the cell pellet depicted on SE MR images, the T2* effect on gradient-echo MR images exceeded the border of the cell pellet and test tube (Fig 4). Therefore, the highest sensitivity for cell detection was obtained with T2*-weighted gradient-echo MR images. They depicted a minimum of 1.0×10^5 cells labeled with magnetic polysaccharide nanoparticles–transferrin, 2.5×10^5 cells labeled with ferumoxides and P7228 liposomes, and 5.0×10^5 cells labeled with ferumoxtran (Fig 2).

In contrast, cell pellets labeled with gadopentetate dimeglumine liposomes showed increased SI on T1-weighted MR images and decreased SI on T2-weighted SE MR images (Fig 4). For these cells, ΔSI data were significantly different on T1- compared with T2-weighted MR images ($P < .05$, Table 2). With use of T1-weighted SE- and T1-weighted gradient-echo MR images, a minimum of 5.0×10^5 cells could be depicted (Fig 2).

Results of follow-up studies showed a normal proliferation of all cell cultures with persistent positive enhancement of gadopentetate dimeglumine liposomes–labeled cells on T1-weighted MR images and gradually decreasing negative enhancement of iron oxide–labeled cells on T2*-weighted MR images up to 7 days after the labeling procedure (Fig 5). Cells labeled with P7228 liposomes, ferumoxides, and magnetic polysaccharide nanoparticles–transferrin showed an inverted increased SI on T1-weighted MR images at day 7 (Fig 5).

DISCUSSION

Results of this study show that human hematopoietic progenitor cells can be labeled with MR contrast agents that are approved by the U.S. Food and Drug Ad-

TABLE 2
Comparison of Results with Iron- and Gadolinium-based Contrast Agents

MR Contrast Agent	T1-weighted SE (500/15)	T1-weighted Gradient Echo (25/2.7 with 40° flip angle)	T2-weighted SE (2,500/90)	T2-weighted Gradient Echo (25/12 with 20° flip angle)
Ferumoxides	−41.2 ± 10.4	−43.1 ± 2.2	−61.8 ± 9.1	−105.6 ± 9.7*
Magnetic polysaccharide nanoparticles–transferrin	−45.3 ± 10.8	−46.7 ± 5.1	−66.8 ± 9.0	−124.0 ± 17.7*
Ferumoxtran	23.0 ± 19.9	24.8 ± 14.9	−58.7 ± 9.1*	−60.6 ± 6.9*
P7228 liposomes	−40.1 ± 10.0	−41.3 ± 8.3	−61.7 ± 9.8	−86.5 ± 9.4*
Gadopentetate dimeglumine	111.4 ± 23.2†	129.9 ± 32.5‡	12.0 ± 9.3‡	4.9 ± 3.1†

Note.—Data are ΔSI. Differences between T1- and T2-weighted pulse sequences and those between iron- and gadolinium-based MR contrast agents were analyzed.
* T1-weighted versus T2-weighted pulse sequences, $P < .05$.
† Gadolinium versus iron, $P < .05$.
‡ Gadolinium versus iron, $P < .01$.

ministration (ferumoxides, gadopentetate dimeglumine) or are being evaluated for approval (ferumoxtran, P7228), and these labeled cells can be visualized in a clinical MR imager with a minimal detectable quantity of 1.0×10^5 cells.

Our results confirm those in previous experimental approaches for cell targeting with iron oxides performed in tumor cells (3), lymphocytes (5,6), neural progenitor cells (2,19), and hematopoietic progenitor cells (2). Numerous studies were focused on the design of new optimized probes with high labeling efficiency to improve MR depiction of labeled cells (2,4,20). However, such new probes become more and more complicated, are not readily available for other researchers, and are not yet approved for clinical applications. In the present study, we focused on simple labeling methods that could be applied in any hospital. We selected labeling probes that are commercially available and potentially applicable in humans.

Though the labeling efficiency of simple incubation with iron oxides is relatively low (3,6), this would be the most feasible technique to be applied for human cells. Ferumoxides and ferumoxtran are designed for cellular uptake; the uptake mechanisms (3,6), subsequent iron metabolism (11), and potential side effects and toxicities have been investigated in humans (11). We optimized this simple incubation method by using two approaches: *(a)* We used progenitor cells from umbilical cord blood. They have higher metabolic, endocytotic, and phagocytic activity compared with those in progenitor cells from bone marrow (2). *(b)* We varied the size of the iron oxide particles because their phagocytic and endocytotic cellular uptake increases with particle diameter. SPIO particles, with a diameter of about 100–150 nm, were more efficient for cell targeting than were monocrystalline iron oxide nanoparticles, or MIONs, and USPIO nanoparticles, which have diameters of 20–40 nm (3,6). Ferumoxides is approved by the U.S. Food and Drug Administration and could be applied in humans. For autologous bone marrow transplantation, a much higher number of cells are administered than were investigated in this study (ie, 2.0×10^8 cells per kilogram, or 140.0×10^8 cells in a 70-kg patient). Further studies are needed to show whether the sensitivity achieved with our labeling method is sufficient for cell detection in vivo.

We applied two methods to increase cell labeling efficiency: *(a)* The attach-

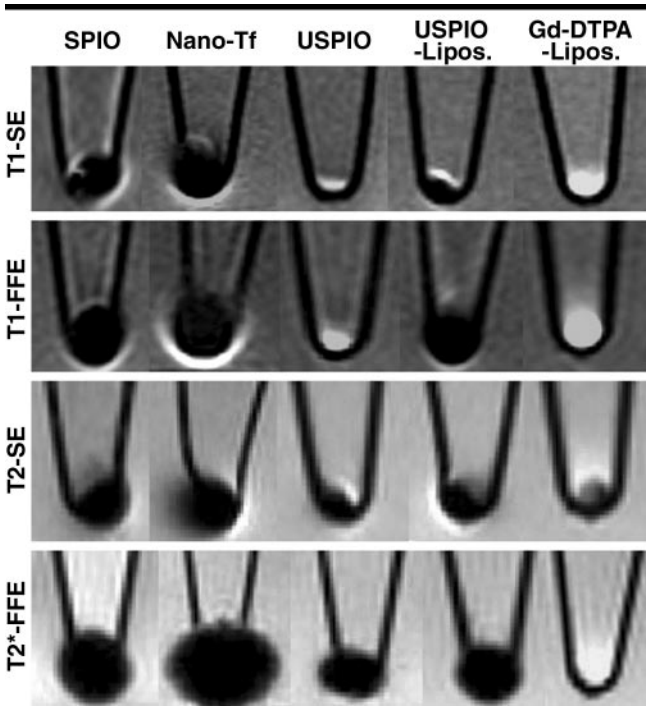

Figure 4. Representative MR images of centrifuged cell pellets in test tubes placed in a water bath. Each cell pellet contains 10^6 cells after exposure to the various contrast agents: *SPIO* = ferumoxides, *Nano-Tf* = magnetic polysaccharide nanoparticles–transferrin, *USPIO* = ferumoxtran, *USPIO-Lipos.* = P7228 liposomes, *Gd-DTPA-Lipos.* = gadopentetate dimeglumine liposomes. Each probe was imaged with the following sequences: T1-weighted SE *(T1-SE)* (500/15), T1-weighted fast field echo *(T1-FFE)* (25/2.7 with 40° flip angle), T2-weighted SE *(T2-SE)* (2,500/90), and fast field echo *(T2*-FFE)* (25/12 with 20° flip angle). Note decreased SI in ferumoxides-labeled cell pellets on T2-weighted images and increased SI in gadopentetate dimeglumine liposomes *(Gd-DTPA-Lipos.)*–labeled cell pellets on T1-weighted MR images. The supernatant above the cells in the test tubes shows identical SI compared with that of the surrounding water bath.

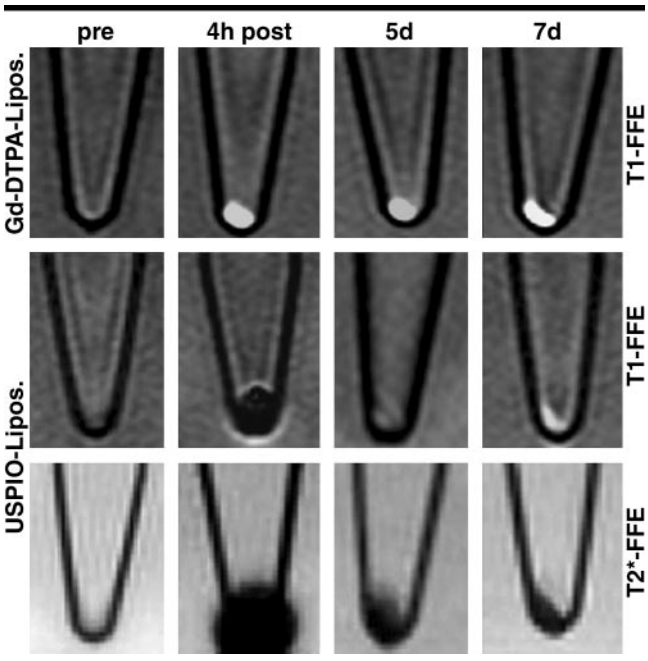

Figure 5. Follow-up MR images of human hematopoietic progenitor cells in test tubes that were obtained before *(pre)* and 4 hours, 5 days, and 7 days after labeling with gadopentetate dimeglumine liposomes *(Gd-DTPA-Lipos.)* or P7228 liposomes *(USPIO-Lipos.)*. Gadolinium-labeled cells show a persistent T1 effect over 7 days, whereas iron oxide–labeled cells show a gradually declining T2 effect. *T1-FFE* = T1-weighted fast field echo, *T2*-FFE* = T2*-weighted fast field echo.

ment of iron oxides to transferrin increased the quantity of iron internalized into progenitor cells. This was also observed for other cell types (21). *(b)* The transfection method provided cellular uptake of gadopentetate dimeglumine, which is usually not phagocytosed. Furthermore, the transfection method can be applied to cells without phagocytic activity (14,22). Our reason for selection of transferrin and liposomes as carriers for the MR contrast agents was that these probes could be applied in human cells. Liposomes are used as carrier systems for cytotoxic drugs (23), gene therapy targets (19,24), and radioactive imaging agents (25). The iron oxides ferumoxides and ferumoxtran could not easily be used for these methods because they have no functionalized group on the dextran coat to facilitate an interaction with other biomolecules. The dextran could be activated for such functionalization (26), but this may impair the stability of the coating. Therefore, we used alternative iron oxides, magnetic polysaccharide nanoparticles and P7228, which have functionalized groups. P7228 will be investigated in clinical trials soon.

For clinical applications, it is desirable to have the choice of depicting labeled cells with either high or low SI on MR images, depending on the background SI of the target organ, where the engraftment of transplanted cells would occur. As a positive contrast agent, one of the small molecular gadolinium chelates approved by the U.S. Food and Drug Administration would be preferred. As shown by our data, the standard contrast agent gadopentetate dimeglumine could be internalized into hematopoietic progenitor cells because the molecule has two negative net charges (one Gd^{3+} group and five COO− groups), which can be associated with positively charged liposomes. Alternatively, the negatively charged gadoterate meglumine (Dotarem; Laboratoire Guerbet, Aulnay-sous-Bois, France) could be used because it has one negative net charge (one Gd^{3+} group and four COO− groups).

A potential limitation of the present study is that the MR contrast agents were administered to the cells in abundance. The minimal quantity of added iron oxides that would provide maximal cellular uptake cannot be calculated from our data because we evaluated the labeling efficiency in the saturation part of the "uptake- versus–added concentration curve." The contrast agent doses were selected on the basis of data from other cell types obtained at our laboratory (unpublished data) and previously reported data about cell labeling with other iron oxides (6) and optimized transfection protocols (14,22).

R2* was measured instead of R2, because the value of R2 depends on the diameter of the iron oxide particle, the diffusion coefficient, and the echo spacing (18). R2* is not dependent on these parameters for particles with a diameter of more than 10 nm (which applies to the iron oxides investigated in the present study). Moreover, the SI of the cell probes on the pulse sequences is mainly determined by the R2* effect of the iron oxides.

We cannot exclude the possibility that multiple mechanisms may have contributed to the cellular uptake of each contrast agent. Previous investigators found that the main cellular uptake mechanism is phagocytosis and fluid-phase endocytosis for both SPIO and USPIO (3,6), receptor-mediated endocytosis for transferrin-bound iron oxides (21), and transfection for anionic agents entrapped with cationic liposomes (22–25). In the latter two mechanisms, however, additional simple phagocytosis of contrast agent particles may have occurred.

Scintigraphic techniques would provide a much higher sensitivity than that achieved with our MR imaging method. Although the sensitivity of scintigraphy is high, however, the spatial resolution is limited, and radiotoxic cell damage could occur (27).

Results of follow-up studies showed a persistent MR enhancement of labeled cultured progenitor cells for at least 7 days. The iron oxide–labeled cells showed a gradual decline of the susceptibility effect with increasing time after the labeling process. This may be explained by the well-known progressive iron oxide metabolism and subsequent vanishing of iron quantity within the cells (11). The inversion of the SI on T1-weighted images may be a result of changes in the molecular structure of the iron oxide particles: The dextran coat undergoes progressive degradation, and iron oxide particles are released from the iron oxide core. These can freely interact with water protons through an outer-sphere mechanism and thereby provide a T1 effect (9–11). On the other hand, cells labeled with gadopentetate dimeglumine did not show any decline in SI up to 1 week after the labeling process. This may be due to a lack of metabolism of this chelate (12,13). The coating with liposomes might prevent the diffusion of the agent back into the extracellular space. Further

studies are needed to define the interval to the time that iron oxide– and gadolinium-labeled progenitor and stem cells can be detected in vivo. Findings in previous studies with other cell types show detectable in vivo MR enhancement of iron oxide–labeled lymphocytes up to 48 hours (6) and of iron oxide–labeled neural progenitor cells up to 42 days (19).

In the present study, no impairment of cell vitality or proliferation was observed up to 7 days after the labeling procedure. Further in vivo studies about the biology of labeled umbilical cord cells in mice are in progress at our institution. Previous in vivo investigations of hematopoietic progenitor cells from the peripheral blood and neural progenitor cells did not show any impairment of cell viability, differentiation, proliferation, and biodistribution due to labeling with iron oxides (2,19).

In summary, findings in this study show that human hematopoietic progenitor cells can be labeled with MR contrast agents that are approved by the U.S. Food and Drug Administration or those that are being evaluated for approval. Thus, these probes are either readily applicable or will become available for clinical applications in the near future. Future studies at our institution will focus on the clinical application of these new techniques.

Practical applications: Potential practical applications of these labeling methods include MR depiction and follow-up studies of autologous and allogeneic bone marrow transplantation (1), stem cell transplantation to repair and regenerate injured myocardium (28), natural killer cell accumulation in tumors during therapy (29), and tracking of genetically engineered progenitor cells (24). Potential applications for stem cell transplantation include in vivo tracking of stem cell subtypes or manipulated stem cells to modulate homing specificity and assessment of therapy effects on stem cell differentiation outcomes (2).

Acknowledgments: We thank Claire Corot, PhD, from Laboratoire Guerbet for providing the iron oxide contrast agents and for her advice and discussions concerning the study design and data analyses. We thank Luise Jennen, MS, from the National Research Center for Environment and Health, Technical University of Munich, Germany, for her help with the processing of cell samples for electron microscopy. We thank Raymonde Busch, Dipl Math, from the Institute of Medical Statistics, Technical University of Munich, for her help with the statistical analyses.

References

1. Molina A, Popplewell L, Kashyap A, Nademanee A. Hematopoietic stem cell transplantation in the new millennium: report from City of Hope National Medical Center. Ann N Y Acad Sci 2001; 938: 54–61.
2. Lewin M, Carlesso N, Tung CH, et al. Tat peptide-derivatized magnetic nanoparticles allow in vivo tracking and recovery of progenitor cells. Nat Biotechnol 2000; 18:410–414.
3. Weissleder R, Cheng H, Bogdanova A, Bogdanov A. Magnetically labeled cells can be detected by MR imaging. J Magn Reson Imaging 1997; 7:258–263.
4. Högemann D, Josephson L, Weissleder R, Basilion J. Improvement of MRI probes to allow efficient detection of gene expression. Bioconjugate Chem 2000; 11:941–946.
5. Yeh T, Zhang W, Ildstad S, Ho C. In vivo dynamic MRI tracking of rat T-cells labeled with superparamagnetic iron oxide particles. Magn Reson Med 1995; 33:200–208.
6. Schoepf U, Marecos E, Melder R, Jain R, Weissleder R. Intracellular magnetic labeling of lymphocytes for in vivo trafficking studies. Biotechniques 1998; 24:642–651.
7. Weissleder R, Elizondo G, Wittenberg J, Rabito C, Bengele H, Josephson L. Ultrasmall superparamagnetic iron oxide: characterization of a new class of contrast agents for MR imaging. Radiology 1990; 175:489–493.
8. Weissleder R. Liver MR imaging with iron oxides: toward consensus and clinical practice. Radiology 1994; 193:593–595.
9. Jung CW. Surface properties of superparamagnetic iron oxide MR contrast agents: ferumoxides, ferumoxtran, ferumoxsil. Magn Reson Imaging 1995; 13:675–691.
10. Chambon C, Clement O, Le Blanche A, Schouman-Claeys E, Frija G. Superparamagnetic iron oxides as positive contrast agents: in vitro and in vivo evidence. Magn Reson Imaging 1993; 11:509–519.
11. Weissleder R, Stark D, Engelstad B, Bacon B, Compton C. Superparamagnetic iron oxide: pharmacokinetics and toxicity. AJR Am J Roentgenol 1989; 152:167–173.
12. Weinmann H, Brasch R, Press W, Wesbey G. Characteristics of gadolinium-DTPA complex: a potential new NMR contrast agent. AJR Am J Roentgenol 1984; 142: 619–624.
13. Weinmann H, Laniado M, Mützel W. Pharmacokinetics of Gd-DTPA/dimeglumine after intravenous injection into healthy volunteers. Physiol Chem Phys Med NMR 1984; 16:167–172.
14. Felgner P, Gadek T, Holm M, et al. Lipofectin: a highly efficient, lipid mediated DNA-transfection procedure. Proc Natl Acad Sci U S A 1987; 84:7413–7417.
15. Daldrup-Link HE, Rummeny EJ, Ihssen B, Kienast J, Link TM. Iron-oxide-enhanced MR imaging of bone marrow in patients with non-Hodgkin's lymphoma: differentiation between tumor infiltration and hypercellular bone marrow. Eur Radiol 2002; 12:1557–1566.
16. Wolff S, Balaban R. Assessing contrast on MR images. Radiology 1997; 202:25–29.
17. In den Kleef JJE, Cuppen JJM. RLSQ: T1, T2 and rho calculations, combining ratios and least squares. Magn Reson Med 1987; 5:513–524.
18. Gillis P, Moiny F, Brooks RA. On T2-shortening by strongly magnetized spheres: a partial refocusing model. Magn Reson Med 2002; 47:257–263.
19. Bulte J, Douglas T, Witwer B, et al. Magnetodendrimers allow endosomal and in vivo tracking of stem cells. Nat Biotechnol 2001; 19:1141–1147.
20. Josephson L, Tung CH, Moore A, Weissleder R. High-efficiency intracellular magnetic labeling with novel superparamagnetic-tat peptide conjugates. Bioconjugate Chem 1999; 10:186–191.
21. Bogdanov A, Weissleder R. The development of in vivo imaging systems to study gene expression. Trends Biotechnol 1998; 16:5–10.
22. Felgner P, Ringold G. Cationic liposome-mediated transfection. Nature 1989; 337: 387–388.
23. Lasic D, Papahadjopoulos D. Liposomes revisited. Science 1995; 267:1275–1276.
24. Felgner P, Tsai Y, Sukhu L, et al. Improved cationic lipid formulations for in vivo gene therapy. Ann N Y Acad Sci 1995; 772:126–139.
25. Boerman O, Storm G, Oyen W. Sterically stabilized liposomes labeled with indium-11 to image focal infection. J Nucl Med 1995; 36:1639–1644.
26. Kresse M, Wagner S, Pfefferer D, Lawaczeck R, Elste V, Semmler W. Targeting of ultrasmall superparamagnetic iron oxide (USPIO) particles to tumor cells in vivo by using transferrin receptor pathways. Magn Reson Med 1998; 40:236–242.
27. Fawwaz R, Oluwole T, Wang N, et al. Biodistribution of radiolabeled lymphocytes. Radiology 1985; 155:483–486.
28. Orlic D, Kajstura J, Chimenti S, et al. Bone marrow cells regenerate infarcted myocardium. Nature 2001; 410:701–704.
29. Melder R, Brownell A, Shoup T, Brownell G, Jain R. Imaging of natural killer cells in mice by positron emission tomography: preferential uptake in tumors. Cancer Res 1993; 53:5867–5871.